

Effect of Crystallographic Orientation on the Pitting Corrosion Resistance of Laser Surface Melted AISI 304L Austenitic Stainless Steel

S. Krishnan, J. Dumbre, S. Bhatt, Esther T. Akinlabi, and R. Ramalingam

Abstract—The localized corrosion behavior of laser surface melted 304L austenitic stainless steel was studied by potentiodynamic polarization test. The extent of improvement in corrosion resistance was governed by the preferred orientation and the percentage of delta ferrite present on the surface of the laser melted sample. It was established by orientation imaging microscopy that the highest pitting potential value was obtained when grains were oriented in the most close-packed [101] direction compared to the random distribution of the base metal and other laser surface melted samples oriented in [001] direction. The sample with lower percentage of ferrite had good pitting resistance.

Keywords—Crystallographic orientation, Ferrite percentage, Laser melting, Pitting corrosion, 304L SS.

I. INTRODUCTION

GOOD corrosion resistance and mechanical properties of 304L SS makes it an ideal candidate material for structural applications in chemical and nuclear reprocessing plants. However, the steel is prone to localized attack like pitting and intergranular corrosion in a sensitized atmosphere and when in contact with corrosive fluids. Earlier studies have proved that wear and corrosion resistance can be improved by laser surface melting without affecting the bulk properties [1]. Laser surface melting improved the corrosion resistance of steels [2], [3]. Chong et al. [4] reported that the corrosion resistance of AISI 304L was improved by laser surface melting which was attributed to the formation of delta ferrite, dissolution or redistribution of precipitates or inclusions and promotion of preferred orientation of δ -austenite along the [2 0 0] direction.

Arash Shahryari et al. [5] showed that in 316 low carbon vacuum melted (316 LVM) steels the pitting corrosion susceptibility of the grains is dependent on the orientation of the crystallographic planes parallel to the surface. The planes {111} and {100} have the highest resistance to pitting

corrosion and generally a lower pitting resistance is expected for the crystallographic planes with lower atomic density. Ravikumar et al. [6] showed the presence of close pack crystallographic planes parallel to the specimen surface improved the corrosion properties. Wang et al. [7] showed an increase in the extent of the preferred orientation of austenite along [200] direction in laser melted AISI 321 austenitic stainless steel increased the pitting corrosion resistance. Hence, there are individual studies to show that laser melting induce preferred orientation and preferred orientation increases the pitting corrosion resistance. The studies showing the preferred orientation by orientation imaging microscopic studies (OIM) on laser melted alloys are few [3], [5]. Earlier studies quantified the amount of delta ferrite formed after laser melting by XRD studies [7]. The quantification by XRD is not accurate as XRD can only give the amount of delta ferrite formed in the bulk sample and not on the surface. Hence, the present study is taken to quantify the amount of delta ferrite formed on the surface of laser melted sample by orientation imaging microscopy and to show the effect of crystallographic orientation on the pitting corrosion resistance of laser melted AISI 304L SS.

II. EXPERIMENTAL PROCEDURE

The material used in this study was a rolled AISI 304L SS with the nominal composition of (wt. %) C-0.027, Ni-8.11, Cr-18.33, Si-0.38, P-0.032, S-0.017, Mn-1.35, N-0.056. The dimensions of the plate used for the study was 150mmx150mmx5mm. Prior to laser melting, the plates were cleaned with acetone and then grit blasted with alumina at 6 bar pressure to increase the laser absorption. Laser surface melting was carried using a continuous wave 1kW Nd: YAG laser with a beam diameter of 600 μ m. There was 50% overlap between subsequent passes to obtain a laser surface melted area of 1cm². Samples were laser surface melted by varying the laser power (500, 600, 800W) at a constant laser scan velocity of 300mm/min. All other parameters remained constant. Software based Princeton Applied Research (PAR) basic electrochemical system was used to conduct potentiodynamic polarization tests. A conventional three electrode cell was used for the corrosion study and laser melted AISI 304L was used as a working electrode, platinum is used as auxiliary electrode and saturated calomel electrode as reference electrode. 3.5% NaCl was used as an electrolyte at room temperature and tests were conducted at a scan rate of 1mV/s.

K. Surekha was with the Indian Institute of Technology Mumbai, India. She is now with the University of Johannesburg, P.O. Box 524, Auckland Park, Johannesburg 2006, South Africa. (phone:+27 559 2103; fax:+27 559 2532 ; e-mail:surekhakrishnan2020@gmail.com)

Jayshri Dumbre was with the Indian Institute of Technology Mumbai, India. She is now with Crompton Creaves, Mumbai, India. (phone:+91 9930977322)

Swetha B. was with the Indian Institute of Technology Mumbai, India. Unfortunately, she is not with us today.

E. T. Akinlabi is with the University of Johannesburg. P.O. Box 524, Auckland Park, Johannesburg 2006, South Africa. (e-mail: etakinlabi@uj.ac.za).

R. Raman is with the Indian Institute of Technology Mumbai, India.

Orientation imaging microscope (OIM) studies were performed on the samples to find the orientation of the grains and the amount of different phases present in laser melted zone (LMZ) using a Fei Quanta 200 HV SEM with TSL-EDX orientation imaging microscopy (OIM).

III. RESULTS AND DISCUSSION

Table I shows the parameters used for laser surface melting along with their nomenclature.

TABLE I
PARAMETERS USED FOR LASER MELTING

S.No	Name	Power (W)	Scan velocity (mm/min)
1.	Basemetal (BM)	-	-
2.	LP	500	300
3.	MP	600	300
4.	HP	800	300

A. Microstructural Characterization

Fig. 1 shows the SEM images of the HP laser melted sample and the base metal.

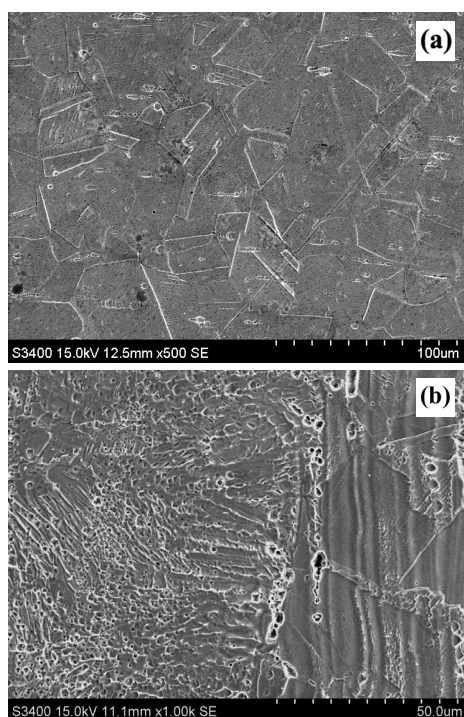


Fig. 1 SEM images of (a) BM and (b) HP

The base metal showed austenitic grain structure along with the twin boundaries. In the laser melted samples, dendritic structure was observed. At the fusion boundary, a thin layer of cellular grains was noticed and then the grain structure changed rapidly to dendritic structure. Just after the fusion boundary, large elongated dendritic structure was noticed. The dendritic structure was very coarse as the cooling rate was slow at higher power and there was enough time for grain growth.

B. Effect of Crystallographic Orientation

Figs. 2-5 shows the inverse pole figure maps and phase analysis maps of the BM, LP, MP and HP laser melted samples. In Fig. 2, it was noticed from the color codes obtained from OIM map that the orientation of the grains was random in nature in the base metal. This indicated the weak texture of the base metal and the texture index was found as 1.42147. In the laser melted samples, preferred orientation was observed. In HP and LP samples, the orientation was in the [001] direction. In MP sample, the grains were oriented in the [101] direction. The texture indexes of laser melted samples are shown in Table II.

C. Distribution of Delta Ferrite

The amount of delta ferrite formed on the surface of laser melted samples was determined by OIM studies. The summary of OIM studies is tabulated in Table II. It can be noticed in Figs. 3-5, that dendritic grains are coarser in HP samples compared to LP and MP samples. This is attributed to the high power used and hence the lower cooling rate obtained [8]. The percentage of delta ferrite present determined the distribution of the ferrite in the matrix [9]. It can be seen in Figs. 2 and 4 that the delta ferrite is distributed as isolated cores and in Fig. 3 as discontinuous network and in Fig. 5 as continuous network. This variation in morphology of the delta ferrite is attributed to the 0.5%, 7.0%, 2.1% and 38.6% of ferrite present in BM, LP, MP and HP samples respectively.

D. Effect of Pitting Resistance

Formation of delta ferrite less than 5% is conducive to the pitting resistance and greater amounts deteriorate the pitting resistance. This can be attributed to the higher pitting potential of 663mV in MP sample as the delta ferrite content is 2.1%. The lower pitting resistance of 122mV of the HP sample is because of 38.6% delta ferrite present in the sample. The potential difference between ferrite and austenite and the distribution of ferrite as continuous network further accelerated the pitting in HP sample. The composition of microconstituents, their size, quantity, location, continuity and corrosion potential relative to the adjacent matrix affects the corrosion behavior [10].

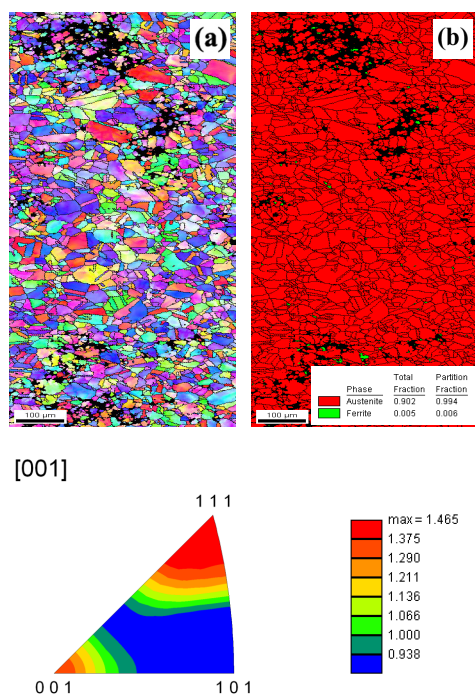


Fig. 2 (a) Inverse Pole figure map and (b) phase analysis of BM

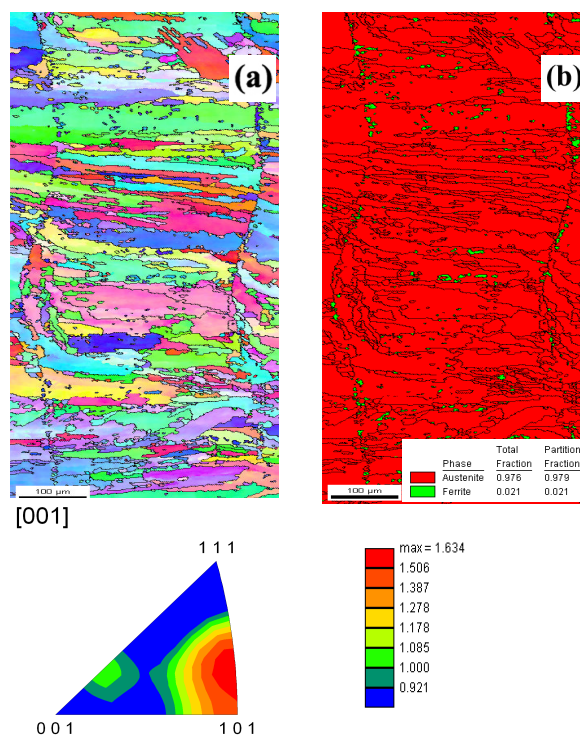


Fig. 4 (a) Inverse Pole figure map and (b) phase analysis of MP

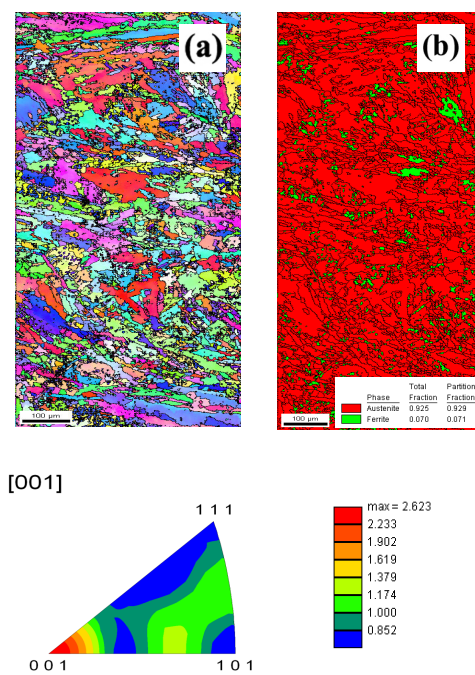


Fig. 3 (a) Inverse Pole figure map and (b) phase analysis of LP

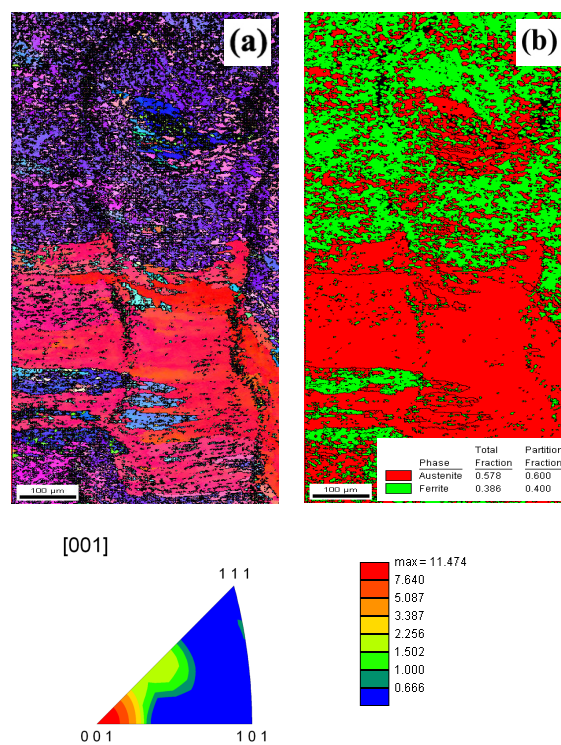


Fig. 5 (a) Inverse Pole figure map and (b) phase analysis of HP

TABLE II
PITTING POTENTIAL, PERCENTAGE OF FERRITE, TEXTURE INDEX AND CRYSTALLOGRAPHIC ORIENTATION OF BM AND LASER MELTED SAMPLE

Name	Pitting potential (mV)	Crystallographic Orientation	Texture Index	Surface δ -Ferrite (%)	Austenite (%)
BM	213	Random	1.42147	0.5	90.2
LP	452	[001]	2.21112	7.0	92.5
MP	663	[101]	3.49994	2.1	97.6
HP	122	[001]	35.0758	38.6	57.8

IV. CONCLUSIONS

It has been found that laser melting improved the corrosion resistance of the AISI 304 L SS and orientation microscopy determined the exact amount of delta ferrite present on the surface. Higher amount of delta ferrite formation has detrimental effect on the pitting corrosion resistance. Preferred orientation in closed packed direction improves corrosion resistance.

REFERENCES

- [1] O. V. Akgun, O. T. Inal, M. L. Lovato, and T. R. Jervis, "Effect of laser surface melting on tensile properties of type 304L stainless steel," *Scripta Metallurgica et Materialia*, Vol. 27, no.2, pp. 191-194, July 1992.
- [2] A. Conde, I. Garcia, J. J. de Damborenea, "Pitting corrosion of 304 stainless steel after laser surface melting in argon and nitrogen atmospheres," *Corrosion Science*, Vol. 43, pp. 817-828, 2001.
- [3] T. M. Yue, J. K. Yu, H. C. Man, "The effect of excimer laser surface treatment on pitting corrosion resistance of 316LS stainless steel," *Surface and Coatings Technology*, Vol. 137, pp.65-71, 2001
- [4] P. H. Chong, Z. Liu, X. Y. Wang, P. Skeldon, "Pitting corrosion behaviour of large area laser surface treated 304L stainless steel," *Thin Solid Films*, Vol. 453, pp.388-393, 2004.
- [5] A. Shahryari, J.A. Szpunar, S.Omanovic, "The influence of crystallographic orientation distribution on 316LVM stainless steel pitting behaviour," *Corrosion Science*, Vol. 51 pp.677-682, 2009.
- [6] B. Ravi Kumar, R.Singh, B. Mahato, P. K. De, N. R. Bandyopadhyay, D. K. Bhattacharya, "Effect of texture on corrosion behaviour of AISI 304L stainless steel," *Materials Characterization*, Vol. 54 pp.141- 147, 2005.
- [7] X. Y. Wang, Z. Liu, P. H. Chong, "Effect of overlaps on phase composition and crystalline orientation of laser-melted surfaces of 321 austenitic stainless steel," *Thin Solid Films*, Vol. 453, pp.72-75, 2004.
- [8] W. Hofmeister, M. Wert, J. Smugeresky, J.A. Philliber, M. Griffith, and M. Ensz, "Investigating Solidification with the Laser-Engineered Net Shaping (LENSTM) Process," *JOM-e*, vol.51, no.7. <http://www.tms.org/pubs/journals/jom/9907/hofmeister/hofmeister-9907.html>
- [9] A. F. Padilha, C. F. Tavares; M. A. Martorano, "Delta Ferrite Formation in Austenitic Stainless Steel Castings," *Materials Science Forum*, Vol. 730-732, pp 733-738, 2013.
- [10] E.H. Dix, "Corrosion of light metals," *American Society of Metals*, 15, 1946.